

## Journal of Molecular Science

www.jmolecularsci.com

ISSN:1000-9035

Formulation Of Nanosponges Containing Isolated Compound Of *Launaea Pinnatifida* Against Wound Healing ActivityAnnapurna Ojha<sup>1\*</sup>, Rajendra Pal Singh Rathore<sup>2</sup><sup>1</sup>Research Scholar, Faculty of Pharmacy, Bhupal Nobles' University, Udaipur, Rajasthan, India.<sup>2</sup>Associate Professor, Faculty of Pharmacy, Bhupal Nobles' University, Udaipur, Rajasthan, India.**Article Information**

Received: 11-08-2025

Revised: 21-08-2025

Accepted: 02-09-2025

Published: 17-09-2025

**Keywords***Launaea pinnatifida*,  
*nanosponges*, *Box-Behnken*  
*design*, *wound healing*  
*activity*, *acute dermal toxicity*,  
*antimicrobial activity* etc**ABSTRACT**

The present study focuses on the formulation and evaluation of nanosponges containing an isolated compound from *Launaea pinnatifida* (LP) for wound healing activity. LP, a member of the Asteraceae family, is known for its anti-inflammatory, antioxidant, and antimicrobial properties. Fraction G of LP extract was isolated through column chromatography and characterized using UV-visible spectroscopy, showing a  $\lambda_{max}$  at 327 nm. The nanosponge formulation was optimized using a Box-Behnken design, with ethyl cellulose and polyvinyl alcohol as key excipients. The optimized nanosponges demonstrated a particle size of 244.6 nm, zeta potential of  $-15$  mV, drug entrapment efficiency of 82.4%, and percentage yield of 90%. SEM confirmed spherical morphology with porous structure, while the nanosponge-loaded gel exhibited favorable physical properties, pH ( $7.1 \pm 0.027$ ), spreadability, viscosity, and stability over six months. Antioxidant assays revealed significant free radical scavenging and reducing power activity. Antimicrobial studies showed inhibitory effects against *E. coli* and *S. aureus*. Acute dermal toxicity studies confirmed safety with no adverse effects. In vivo wound healing studies in Wistar rats demonstrated accelerated wound contraction (98.86% by day 21) in the nanosponge gel group, comparable to the standard Cipladine gel. These findings indicate that LP-derived nanosponge gel enhances wound healing efficacy through sustained release and synergistic bioactive properties, offering a promising phytopharmaceutical approach for managing wounds.

**©2025 The authors**

This is an Open Access article distributed under the terms of the Creative Commons Attribution (CC BY NC), which permits unrestricted use, distribution, and reproduction in any medium, as long as the original authors and source are cited. No permission is required from the authors or the publishers. (<https://creativecommons.org/licenses/by-nc/4.0/>)

**1. INTRODUCTION:**

Nanotechnology has a versatile use in the field of disease therapy, targeted drug delivery, biosensing, and environmental protection. Nanoparticles have unique properties at their submicron size scale and can be engineered to carry out specific biomedical functions. On the other hand, there are various green synthesis routes available for the synthesis of nanoparticles using natural products (Khosravi-Darani et al., 2019; Habtemariam and Kereta, 2020). Nanosponges (NSs) are an innovative concept for the delivery of drugs. They are nanosized sponge-like structures consisting of numerous cavities that can be filled with payloads.

These polymeric sponge-like structures can accommodate both the lipophilic and hydrophilic drugs, and they offer the improved aqueous

solubility to poorly soluble drugs with improved bioavailability (Girigswami et al., 2022).

Wound healing is a complex and dynamic biological process involving sequential cellular and molecular events directed toward tissue regeneration and repair. It progresses through four overlapping phases: hemostasis, inflammation, proliferation, and remodeling (Gurtner et al., 2008). Despite advances in wound care management, chronic and non-healing wounds remain a major clinical challenge, necessitating novel therapeutic approaches. Natural bioactive compounds derived from medicinal plants have gained attention due to their anti-inflammatory, antimicrobial, and antioxidant properties, which can accelerate wound healing (Anand et al., 2022).

*Launaea pinnatifida* (LP), a member of the Asteraceae family, is traditionally known for its pharmacological properties, including anti-inflammatory, antioxidant, and antimicrobial activities (Sahu et al., 2018). Phytochemical studies have identified flavonoids, phenolics, terpenoids, and alkaloids in LP, which contribute to its therapeutic effects (Kumar et al., 2020). However, the isolation and characterization of the specific bioactive constituents responsible for its wound healing potential remain limited. Chromatographic techniques, such as Thin Layer Chromatography (TLC) and Column Chromatography (CC), are widely employed for isolating and purifying active compounds from plant extracts (Khan et al., 2021). Spectroscopic methods, including UV-Vis, Fourier Transform Infrared (FT-IR), Nuclear Magnetic Resonance (NMR), and Mass Spectrometry (MS), further support structural elucidation (Patel et al., 2022; Zia et al., 2020).

Formulation strategies such as nanosponges and hydrogel-based delivery systems have shown promise in enhancing the bioavailability and therapeutic efficacy in wound healing (Anjali et al., 2022).

Therefore, the present investigation focuses on the isolation, characterization, and pharmacological evaluation of bioactive compounds from LP, with special emphasis on their wound healing potential using in vivo models. The study aims to contribute to the growing evidence on plant-derived therapeutics and explore nanosponge-based delivery systems as a novel approach for improving wound healing outcomes.

## **MATERIAL AND METHOD:**

### **Extraction:**

*Launaea pinnatifida* plants were collected from the local area of Bhopal. The plants were shade-dried,

and extraction was performed using hydroalcohol (70% ethanol) by the Soxhlet method.

### **Anti-oxidant Activity:**

#### **• DPPH free radical scavenging activity**

The free radical scavenging activity of extracts were evaluated by the 2,2-diphenyl-1-picryl-hydrazyl (DPPH) method in which the electron-donating capacity of the extract was calculated from the bleaching of the purple-colored DPPH solution dissolved in methanol. This spectrophotometric assay uses DPPH as a stable reagent (Jena et al., 2017). A solution was prepared by dissolving 0.1mM of DPPH in 100mL of methanol. The sample of different concentrations (20–100 µg/mL) was prepared in methanol in different tubes and was mixed with 2 mL of DPPH solution. Then, the reaction mixture was vortexed properly and left for 30 min in dark. A control sample containing 1 mL of methanol with 2 mL of DPPH solution was used to measure the maximum DPPH absorbance. The absorbance of the mixture was measured by spectrophotometer at 517 nm. Ascorbic acid was used as the reference (Jena et al., 2017). Results were expressed as percentage of inhibition of the DPPH radical according to the following equation:

$$\% \text{ Inhibition} = \left[ \frac{\text{Ab of control} - \text{Ab of sample}}{\text{Ab of control}} \times 100 \right]$$

#### **• Reducing power assay**

Reducing power of extracts was measured by method of (Bursal, and Köksal, 2011). According to this method, the reduction of Fe<sup>3+</sup> to Fe<sup>2+</sup> was determined by measuring absorbance of the Perl's Prussian blue complex. This method is based on the reduction of (Fe<sup>3+</sup>) ferricyanide in stoichiometric excess relative to the antioxidants. For this purpose, different concentrations (20-100 µg/ml) of extracts in distilled water were mixed with 2.5ml of 0.2 M sodium phosphate buffer (pH 6.6) and 2.5ml (1%) of potassium ferricyanide [K<sub>3</sub>Fe (CN)<sub>6</sub>]. The mixture was incubated at 50 °C for 20 min. After 20 min of incubation, the reaction mixture was acidified with 2.5 ml of trichloroacetic acid (10%). The upper layer of solution 2.5 ml was mixed with 2.5 ml distilled water. Finally, 0.5 ml of FeCl<sub>3</sub> (0.1%) was added to this solution. Distilled water was used as blank and for control. Absorbance of this mixture was measured at 700 nm using a UV spectrophotometer. Decreased absorbance indicates ferric reducing power capability of sample.

#### **Thin layer chromatography:**

Solvent system developed in preliminary TLC for LP extract in which the maximum spots were visible in Toluene: Ethyl acetate: Acetic acid (8:2:0.5) mobile phase with std. Flavonoid. So that Toluene:

Ethyl acetate: Acetic acid (8:2:0.5) solvent was taken as mobile phase for column chromatography.

**Column chromatography:**

Hydroalcoholic extract was subjected to silica gel column chromatography for isolation of LP extract. Column was packed using wet packing technique using silica gel (60-120) as the adsorbent. Slurry was prepared using toluene and was poured in to the column. 1gm of extract was added over the top of the column. Gradient elution technique was followed for column chromatography. The column was eluted with Toluene: Ethyl acetate: Acetic acid (8:4:0.5) number of elutes were collected. The fractions/elutes collected were concentrated and TLC was performed to identify the presence of single compound (Srivastava *et al.*, 2021).

**UV-visible Spectroscopy:**

The isolated fraction (G) of LP Extract was scanned from 200 to 800 nm wavelength using UV-Visible Spectrophotometer (Shimadzu UV-1700) and the characteristic peaks were detected and recorded (Patel *et al.*, 2022).

**Formulation and development:**

**Optimization of nanosponges via Box Behnken method (response surface methodology)**

The experimental nature based on this mixture of the component has resulted in 17 separate nanosponge formulation batches. As indicated, numerous nanosponge lots were prepared and then assessed for each of the responses. The responses observed were fit to 17 runs, and it has been noted that the best fit model was the quadratic model for the two dependent variables. The significance of the model with that of comparing with the other model for the analysis by analysis of variance (ANOVA). The present investigation utilized a 32 complete factorial design. The design considered two factors, which were assessed at 3 levels: high (1), medium (0), and low (-1). Independent variables chosen were EC ratio (X1), PVC (X2) and (X3) stirring time. The dependent variables chosen were the particle size (Y1), and entrapment efficiency (Y2) (Ahmed *et al.*, 2021).

**Optimized formula:**

For the preparation of nanosponge solvent diffusion method was used. This method uses different proportion of ethyl cellulose and polyvinyl alcohol. The dispersed phase containing ethyl cellulose and drug was dissolved in 20 ml dichloromethane and slowly added to a definite amount of polyvinyl alcohol (1.5% w/v) in 100 ml of aqueous continuous phase. The reaction mixture was stirred at 1500 rpm for 2hrs. Then nanosponge formed were collected by filtration and dried in the oven at 40° C for 24 hrs. The dried nanosponge was stored in vacuum

desiccators to ensure residual solvent was evolved (Osmani *et al.*, 2015).

**Table 1 Optimized nanosponges formulation**

S. No	Formulation code	Chemical constituents	Quantity	Phase
1	NMF	Drug	5 mg	Internal phase
2		Ethyl cellulose	6.5 mg	Internal phase
3		DCM	20 ml	Internal phase
4		PVA in Distilled water	1.5% w/v (1.5 gm) Up to 100 ml	External phase

**Evaluation parameters of optimized formulation Percentage Yield:**

The percentage yield of several batches of 1.5% w/v was determined by applying the following formula, which involved utilizing the weight of the finished product after drying [practical mass] in relation to original total weight of medication as well as the polymer that was utilized for the creation of NMF [theoretical mass] (Danaei *et al.*, 2018):

$$\text{Percentage yield} = (\text{Practical mass/theoretical mass}) \times 100$$

**Particle Size and Polydispersity Index**

Particle size (z-average diameter) and Poly Dispersity Index (as a measure of particle size distribution) of drug loaded Nanosponge dispersion was performed by dynamic light scattering also known as photon correlation spectroscopy (PCS) using a Malvern Zetasizer (Malvern Instruments, UK) at 25°C7.

**Zeta Potential:**

For Zeta Potential determination, 1ml of sample of nanosponges suspension was filled in clear disposable zeta cell, without air bubble within the sample, the system was set at 25°C temperature, an electric field of about 15 V/cm and results was recorded. The more negative zeta potential indicates more stable Nanosponge formulation.

**Determination of Drug Entrapment Efficiency:**

**Entrapment efficiency was determined using the dialysis method:** The entrapment efficiency of the nanosponge formulation was determined using the dialysis method. A cellophane membrane was used as a semipermeable barrier. Prior to use, the membrane was soaked in a glycerol:water mixture (1:3 v/v) for 15 min to improve flexibility and permeability. The pretreated membrane was tied at one end of an open-ended glass tube. An accurately weighed amount of nanosponge formulation (100 mg) was placed inside the membrane. The tube was then immersed in 100 ml of phosphate buffer saline (PBS, pH 6.8) as the receptor medium, which

provide conditions similar to the physiological environment. The system was continuously stirred using a magnetic stirrer to ensure uniform diffusion. At predetermined time intervals, aliquots of the receptor medium were withdrawn and analyzed spectrophotometrically at 327 nm using a UV-visible spectrophotometer (Shimadzu UV-1700) with PBS as blank. The amount of free (untrapped) drug diffused into the receptor medium was quantified (Alashqar *et al.*, 2017). The entrapment efficiency (EE%) was calculated using the following formula:

$$EE\% = \frac{\text{Total Drug} - \text{Free Drug}}{\text{Total Drug}} \times 100$$

Where; Total drug is Theoretical drug content incorporated in the nanosponge formulation, Free drug is Amount of drug released into the receptor medium (untrapped fraction)

### Morphology of Nanosponge by Scanning Electron Microscopy:

SEM analysis was performed to determine the surface morphology and particle size of the nanosponge formulation. The instrument was operated at an acceleration voltage of 15 kV. An aqueous suspension of the sample was spread onto the specimen holder and dried under vacuum. The dried sample was then coated with a thin gold layer (~20 nm) using a cathodic evaporator to improve conductivity. The coated sample was observed under the SEM, and digital images representing the surface characteristics were captured. From these images, the diameter of multiple individual nanosponges was measured to assess particle size distribution and uniformity.

#### • Nanosponges gel of optimised formulation:

Precisely weighed amount of Carbopol-934 was soaked in water (around 100 mL) for 2 h and neutralized with triethanolamine and stirred continuously. Drug loaded NS (equivalent to topical doses of drugs) were dissolved in polyethylene glycol. This mixture was then transferred to the carbopol mixture and mixing was done for further 20 min. The dispersion was kept aside for 60 min, for complete hydration and swelling of gel components (Moin *et al.*, 2020).

**Table 2 Composition table of optimized nanosponges gel formulation**

S.No	Formulation code	Chemical constituents	Quantity
1	NMFG	Nanosponges (mg)	100
2		Carbapol 940	1% (1gm)
3		Polyethylene glycol	2% (2ml)
4		Triethanolamine	1 ml
5		Methyl paraben	0.001 g
6		Water	50 ml

Evaluation of nanosponges gel (Rahamathulla *et al.*,

2020)

#### • Physical appearance

The physical appearance of the gel was analyzed by the visually and normal human senses. The organoleptic properties included color, odor, and texture.

#### • Determination of pH

Digital pH meter was used to determine pH of the prepared gels.

#### • Homogeneity

After placing the gels in the container, all formulations were tested for homogeneity (aggregates presence and appearance) by inspecting visually.

#### • Spreadability studies

Spreadability is a mean of measuring the extent at which the semisolid formulations gets readily spread onto the administration site post application of little shear. Spreadability of the NS gel formulation was determined using wooden block-glass slide apparatus. Herein, approximately 20 g of weight was applied to upper sliding glass slide and estimation of time needed for complete detachment of upper movable slide from lower fixed slide was done. Higher spreadability is expressed by least time needed for separation of two slides. To calculate spreadability, below formula was used (Tiwari and Bhattacharya, *et al.*, 2022).

$$S = \frac{ML}{T}$$

Where, S = spreadability, M = weight (in grams) tied to upper moving slide, L = length (in cm) of glass slides, and T = time (in sec) taken to separate the two slides completely from each other.

#### • Viscosity studies

All measurements were carried out by viscometer (DV-II+, Brookfield engineering laboratories, Inc., MA, USA) with spindle No. 6 at 10 rpm and at temperature of  $37 \pm 0.5$  °C. The rheological properties of the formulated NS gels were studied at different rpm and the viscosity was recorded in cP.

#### • Stability of the optimized formulation:

As per ICH Guidelines, stability studies were conducted for optimized NS based gel formulation for a period of 6 months and storage conditions were 25 °C/60% RH, 30 °C/60% RH and 40 °C/75% RH. The optimized formulation was analyzed for changes in physical appearance and viscosity at regular time intervals during the study period (Aldawsari *et al.*, 2018).

#### Antimicrobial activity by well diffusion assay

The antimicrobial activity of plant extracts was evaluated using the agar well diffusion method on Nutrient Agar Medium (NAM) and Sabouraud Dextrose Agar (SDA) plates.

**Preparation of NAM:** A total of 28 g of nutrient agar was dissolved in 1 L of distilled water. The pH of the medium was checked and adjusted before sterilization. The medium was autoclaved at 121 °C and 15 lbs pressure for 15 minutes.

**Preparation of SDA:** For SDA, 65 g of dehydrated SDA powder was suspended in distilled water and dissolved by heating with constant stirring. The pH was adjusted to ~5.6, and the medium was sterilized by autoclaving at 121 °C for 15 minutes.

**Inoculum preparation:** The test organisms were grown overnight in broth at 37 °C, and turbidity was adjusted to match 0.5 McFarland standards (corresponding to  $1.5 \times 10^8$  CFU/mL).

**Agar well diffusion assay:** Sterilized media were poured into Petri plates and allowed to solidify under laminar airflow. A sterile cork borer was used to create wells (5–6 mm in diameter) in the agar. Then, 100 µL of the standardized inoculum was spread evenly on the agar surface using a sterile spreader. Three wells were made in each plate and filled with 100 µL of the respective samples: isolated compound, nanosponges, and nanosponge gel. The plates were left at room temperature for 30 minutes to allow diffusion of the samples, followed by incubation at 27 °C for 24 hours. Antimicrobial activity was assessed by measuring the diameter (mm) of the clear zone of inhibition around each well (Kopel et al., 2022).

#### **Acute Dermal Toxicity**

- **Activity I: Acute dermal toxicity study (OECD 402)**

Adult albino rats of Wistar strain weighing almost 150-200g were procured from in-house animal facility of Pinnacle Biomedical Research Institute, Bhopal, India. Animals were acclimatized for up to 7 days for animal house conditions, fed with standard rat feed supplied by Keval Sales Corporation, Vadodara and water ad libitum was provided up to the end of the study. All the experiments were conducted according to the ethical committee norms approved by Ministry of Social Justices and Empowerment, Government of India.

- **Skin preparation for acute dermal toxicity study**

The hairs on the dorsal skin surface (About 6 cm<sup>2</sup>) of animals were carefully shaved 24 hrs using razor

blade before application. Based on OECD guidelines 402, about 10% of the body surface area should be clear for the application of the test substance.

- **Experimental design for acute dermal toxicity**

An intense dermal toxicity test was made in accordance with the guidelines no. 402 given by the OECD for the testing. The dose selection and range-finding study begun with a mid-range dose (200 mg/kg body weight), applying the ointment to a test animal while monitoring for toxicity signs. If severe toxicity occurs, the dose is lowered (e.g., 50 mg/kg), whereas in the absence of toxicity, it is increased (e.g., 1000 or 2000 mg/kg). In the main study, the test chemical was applied uniformly over the exposed skin, covered with gauze, and left for 24 hours. Observations were conducted immediately, periodically within the first 24 hours, and daily for 14 days, assessing changes in skin, fur, eyes, breathing, and behavior, while recording body weight weekly. After 24 hours, any remaining chemical was removed, and the animals were returned to their cages. Necropsy was performed on deceased or sacrificed animals to document visible abnormalities (Anand et al., 2022).

Data on toxicity symptoms, onset time, body weight changes, and mortality were recorded and summarized in tabular form. Toxicity classification followed the GHS acute dermal toxicity guidelines, categorizing the ointment based on LD50 values. No severe toxicity was occurred, a higher dose was tested, whereas if one of two animals dies, a lower dose is evaluated. If both animals die, the substance is classified as highly toxic. Toxicity categories range from highly toxic (LD50 ≤ 50 mg/kg) to unclassified/safe (>2000 mg/kg). The substance was tested using below explanatory diagrammatic representation, each step using three animals of a single sex (Bhavana et al., 2023).

#### **In vivo wound healing**

- **Activity I: Excision Wound healing Activity**

Adult albino rats of Wistar strain weighing almost 150-200g were procured from in-house animal facility of Pinnacle Biomedical Research Institute, Bhopal, India. Animals were acclimatized for up to 7 days for animal house conditions, fed with standard rat feed supplied by Keval Sales Corporation, Vadodara and water ad libitum was provided up to the end of the study. All the experiments were conducted according to the ethical committee norms approved by Ministry of Social Justices and Empowerment, Government of India (Anand et al., 2022).

- **In-vivo wound healing activity**

Total of 24 animals were selected and segregated in

4 groups each containing six animals. They were anaesthetized with slight vapor inhalation of anesthetic ether in anesthesia chamber. The animals' dorsal surfaces were shaved, and a wound with a diameter of roughly approx. 1-2 cm was created by excising the entire skin thickness from the sterile dorsal marked area. Animals were housed in a separate cage according to the groups. The wound continued to be exposed for twenty-one days, each rat's wounds were left open and the standard and test samples were applied topically at a dose of (200mg/rat) once a day. The contraction of wound was expressed as percentage of the reduction in wound size. We calculated the percentage of wound contraction using the following formula.

$$\text{Percentage of wound contraction} = \frac{\text{Initial wound area} - \text{Specific day wound area}}{\text{Initial wound area}} \times 100$$

Table 3 Design of experiment

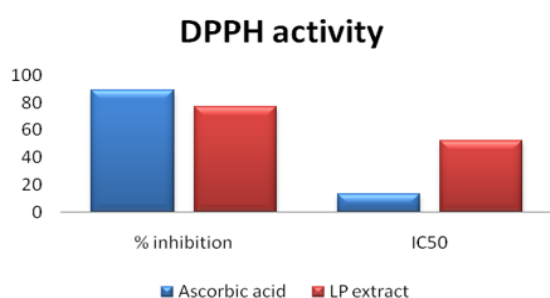
S. No.	Groups	Number of animals	Dose
1	Control	6	Normal Control
2	Inducer	6	Wound treated with placebo
3	Standard	6	1% w/w Cipladine Gel
4	Nanosponges gel	6	1% w/w gel of isolated compound (common name: isolated compound) Nanosponges

## RESULTS:

### Anti-oxidant activity:

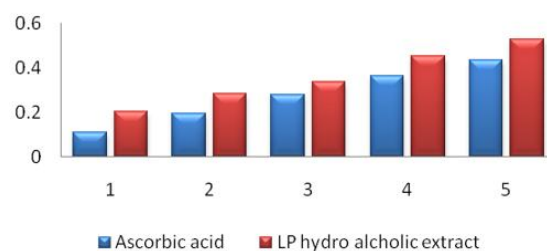
Table 4 DPPH Activity of Ascorbic acid and LP extract

Sample name	% inhibition	IC50
Ascorbic acid	89.285	13.576
LP hydro alcholic extract	77.272	52.41

Figure 1 Graph represents the Absorbance Vs Concentration of Ascorbic acid and Hydroalcoholic extract of *Launaea Pinnatifida*

### • Reducing power scavenging activity

### Reducing power assay

Figure 2 Graph represents the Absorbance Vs Concentration of Ascorbic acid and Hydroalcoholic extract of *Launaea Pinnatifida*

The antioxidant potential of the hydroalcoholic extract of *Launaea pinnatifida* (LP) was evaluated using the DPPH free radical scavenging assay and reducing power activity in comparison with the standard antioxidant, ascorbic acid.

In the DPPH assay (Table 4), ascorbic acid demonstrated a maximum inhibition of 89.28% with an IC<sub>50</sub> value of 13.57 µg/mL, indicating strong radical scavenging capacity. In contrast, the LP hydroalcoholic extract showed 77.27% inhibition with a considerably higher IC<sub>50</sub> value of 52.41 µg/mL. The higher IC<sub>50</sub> value suggests that the extract requires a greater concentration to achieve 50% radical scavenging activity compared to ascorbic acid, implying that while the extract exhibits promising antioxidant activity, its potency is lower than that of the standard.

The graphical representation of absorbance versus concentration further confirms the concentration-dependent increase in scavenging activity for both ascorbic acid and LP extract. However, the slope of the standard curve for ascorbic acid was steeper, reflecting its superior efficiency in neutralizing free radicals.

Similarly, the reducing power assay demonstrated that both the standard and LP extract exhibited increased absorbance with rising concentrations, indicating their electron-donating ability and capacity to reduce Fe<sup>3+</sup> to Fe<sup>2+</sup>. Ascorbic acid again showed a stronger reducing power compared to the LP extract, but the extract's activity still highlights the presence of bioactive phytochemicals, such as phenolics and flavonoids, contributing to its antioxidant potential.

### TLC and Column Chromatography:

TLC of LP extract was performed on different solvent systems (solvent system was selected on the basis of literature survey). TLC performed in Toluene: Ethyl acetate: Acetic acid (8:4:0.5) that were clearly visible bands of LP Extract with Std. Phenol. The R<sub>f</sub> values of LP Extract with Std. Phenol

was found to be 0.49 and 0.49.

The fractions/elutes obtained from silica gel column chromatography of LP extract was tested for the detection of various phyto compounds using TLC.

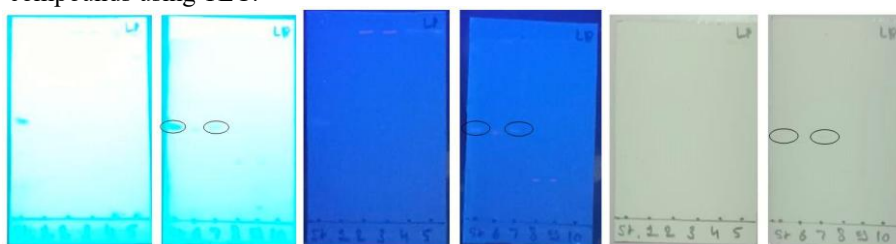


Figure 3 TLC of fractions (A, B, C, D, E, F, G, H, I and J) of LP extract in UV and visible light after column chromatography with Std. Phenol a) Short-UV (254 nm), b) Long-UV (365 nm), c) visible light

Ten elutes (A to J) were collected from column chromatography. Among them, fraction G of the LP extract, eluted with the mobile phase Toluene:Ethyl acetate:Acetic acid (8:4:0.5), showed an Rf value similar to that of standard phenol.

**Spectroscopic characterization of isolated compound:**  
**By UV spectrophotometer:**

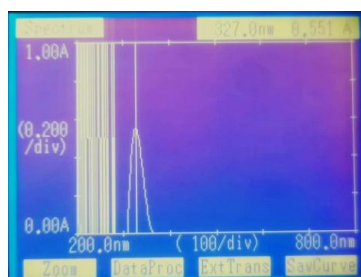


Figure 4 Active constituents estimation By UV- Spectra of (G) fraction of LP extract after column chromatography UV-Spectra of isolated fraction (G) of LP extract were recorded with a Shimadzu 1700 double beam-UV-VIS spectrophotometer. UV spectra of the isolated fraction was recorded in solvent as Toluene: Ethyl acetate: Acetic acid (8:4:0.5) over a scanning range of 200-800 nm and  $\lambda_{max}$  of isolated compound were determined. The Blank was Toluene: Ethyl acetate: Acetic acid (8:4:0.5). The wavelength of isolated fraction (G) of LP extract was found to be one peak at 327 nm.

**Formulation of and development:**

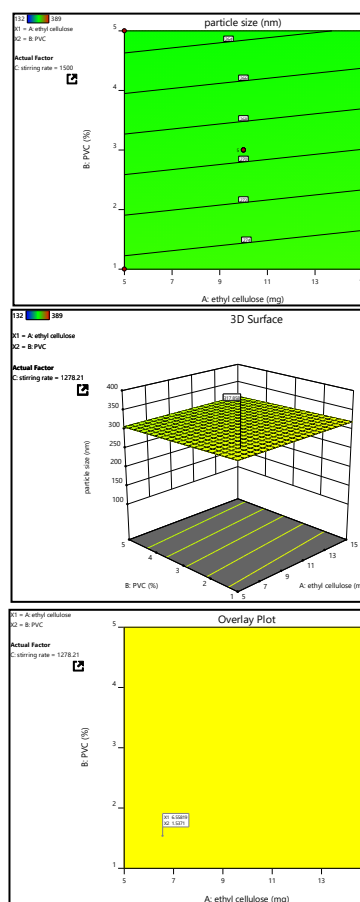


Figure 5 Response surface and Contour plot of particle size dependent variable against independent variables and Overlay plot of particle size dependent variable against independent variables

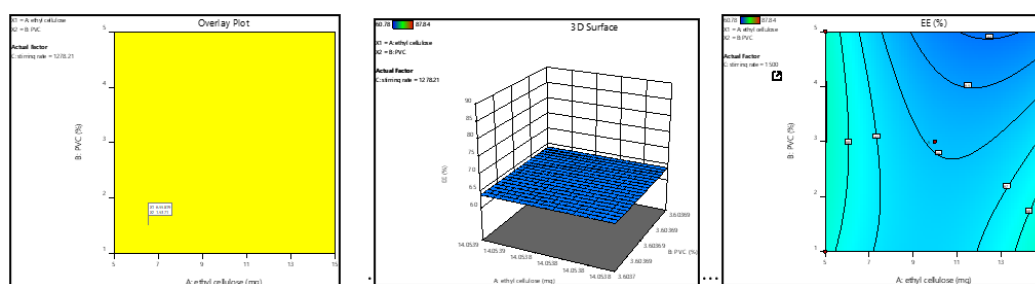


Figure 6 Contour and Response surface plot of entrapment efficiency dependent variable against independent variables and Overlay plot of entrapment efficiency dependent variable

**Data analysis (by Design Expert Software):**

A 32 full factorial design was selected and the 2 factors were evaluated at 3 levels. The amount of Ethyl cellulose (X1) and PVA (X2) were selected as independent variables and the dependent variables were Encapsulation efficiency and % Drug Release. The data obtained was treated using Stat-Ease Design Expert 8.0.7.1 software and analyzed statistically using analysis of variance (ANOVA). The Entrapment efficiency and particle size for 17 batches showed a wide variation.

The present investigation utilized a 32 complete factorial design. The concept involved the evaluation of two elements at three levels: high (1), medium (0), and low (-1). Independent variables selected for analysis were the isolated compound (drug) : EC ratio (X2) in addition to stirring speed (X3) effects. The dependent variables chosen were the particle size (Y1), and entrapment efficiency (Y2).  $Y = b_0 + b_1X_1 + b_2X_2 + b_{12}X_1X_2 + b_{11}X_1^2 + b_{22}X_2^2$  The dependent variable, Y, was represented by an arithmetic mean of 9 runs,  $b_0$ . The estimated coefficient for factor X1 is denoted as  $b_1$ . The primary impacts (X1 as well as X2) indicate the average outcome of altering one element individually from its minimum to maximum value. In statistical analysis, the interaction terms, denoted as  $X_1X_2$ , quantify the effect of changing 2 factors simultaneously on the response variable. Variables  $X_1^2$  and  $X_2^2$  are employed for the analysis of nonlinearity. The analysis of the data demonstrated a significant correlation between the chosen independent variables and the PDI, ZP, and entrapment efficiency values.

**Table 5 Evaluation of optimized formulation**

S. No.	Parameters	Value
1	Percentage yield	90±0.025
2	Particle Size (nm)	244.6
3	Polydispersity Index	34.5%
4	Zeta Potential	-15
5	Drug entrapment efficiency	82.4 ± 0.11 %

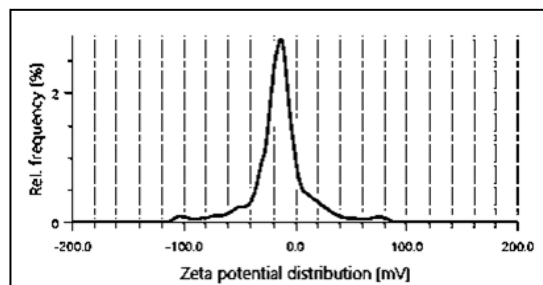
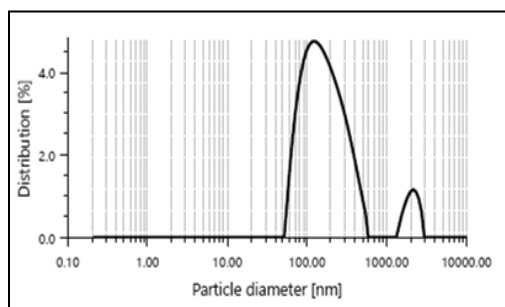


**Figure 7 Particle Size and Polydispersity Index and Zeta Potential of the optimized formulation**

The optimized nanosponge formulation showed a percentage yield of  $90 \pm 0.025\%$ , corresponding to a total quantity of 189 mg. The average particle size was 244.6 nm with a polydispersity index of 0.215, confirming a uniform particle size distribution. The zeta potential, measured using a Malvern Nano Zetasizer, was  $-15$  mV, indicating negatively charged particles that contribute to colloidal stability. The entrapment efficiency (EE) of the optimized formulation was  $82.4\%$ , with results demonstrating that EE varied significantly depending on the drug-to-polymer ratio and was strongly influenced by the amount of crosslinker used.

**Morphology of Nanosponge by SEM**

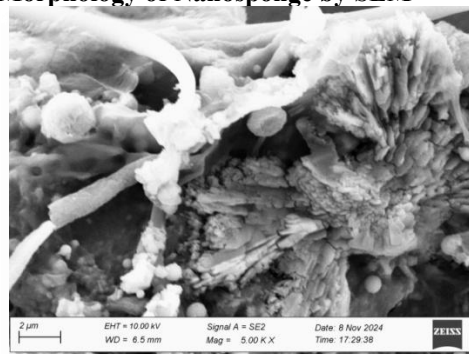


**Figure 8 SEM of the optimized formulation**

SEM analysis was done for the prepared NS to check the morphology and surface texture of the same. As expected, NS were observed to be roughly spherical in shape with uneven surface and spongy nature

**Nanosponges gel of optimised formulation**



**Figure 9 Showing the optimised gel formulation NMFG**

Evaluation of nanosponges gel

Physical appearance

All of the manufactured dermal gel formulations were confirmed to be free of any dispersed particle matter after a thorough visual assessment against a dark and white backdrop. All the formulations were found to be translucent gel. The texture was no greasy and smooth in touch.

Table 6 Represent the physical properties of the optimized gel loaded with drug

S.N.	Formulation code	Parameters	Result
1	NMFG	Color	Translucent (white) in color
		Texture	Smooth
		Appearance	Pleasant
		Odor	Odorless
		Gritty	Non gritty

Table 7 Evaluation parameters of optimized nanosponge-based gel

S. No.	Parameters	Value
1.	pH	7.1 ± 0.027
2.	Homogeneity	Homogenous mixture
3.	Spreadability	31 ± 0.051
4.	Viscosity	2345 cp ± 0.012

The pH of all nanosponge-based gel formulations was recorded as 7.1 ± 0.027, which is within the safety range and close to skin pH. This indicates that the formulations are unlikely to cause skin irritation. All the prepared gels were visually inspected and found to be clear, translucent, and homogenous, without the presence of lumps or aggregates. The formulations also exhibited good spreadability, ensuring ease of application. The viscosity was observed to be 2345 cp ± 0.012, which was

dependent on the polymer concentration in the nanosponge-based gel formulations.

Stability of the optimized formulation

Table 8 Stability study data of NMFG based gel formulation

Stability testing conditions	Sampling interval (months)	Physical appearance	Viscosity *
25 °C /60 ± 5% RH	0	No change	2345 ± 0.32
	3	No change	2355 ± 0.21
	6	No change	2378 ± 0.35
30 °C /60 ± 5% RH	0	No change	2345 ± 0.32
	3	No change	2344 ± 0.52
	6	No change	2348 ± 0.28
40 °C /75 ± 5% RH	0	No change	2345 ± 0.32
	3	No change	2451 ± 0.64
	6	No change	2443 ± 0.52

The optimized formulation's stability indicates a minor shift in viscosity, but this was acceptable.

Antimicrobial activity of samples

Table 9 Anti-bacterial activity of samples

Sample name	<i>E. coli</i>	<i>S. aureus</i>	<i>C. albicans</i>
Isolated compound	8.333 ± 1.527	9.333 ± 0.577	0 ± 0
Nanosponges	11.666 ± 0.577	11.333 ± 0.577	0 ± 0
Nanosponges gel	16 ± 1	15.666 ± 2.081	0 ± 0

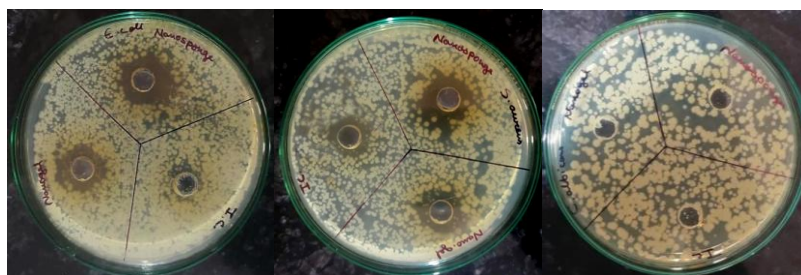


Figure 10 Anti-bacterial activity of samples against *E. coli*, *S. aureus* and *C. albicans*

The antibacterial activity of the isolated compound, nanosponges, and nanosponge-based gel was evaluated against *Escherichia coli*, *Staphylococcus aureus*, and *Candida albicans*. The results (Table and Figure 1) indicate that all three formulations exhibited activity against the tested bacterial strains, while none showed inhibitory effect against the fungal strain *C. albicans* (0 ± 0).

Acute dermal toxicity

There were no changes in skin and fur, eyes, mucous membrane, behaviour patterns, salivation, lethargy,

sleep, diarrhea, coma, and tremors. The observable examples of rats were watched initially 6 hrs and pursued by 24 hrs. The rats in study did not show any critical changes in conduct, skin impacts, breathing, disability in nourishment admission and water utilization, postural variations from the normal state and losing hair.

No mortality was observed during 14 days after the treatment with Nanosponges gel. There were no irritation signs on the skin. This Nanosponges gel should, therefore, be labelling as unclassified

nontoxic in the hazard category according to Globally Harmonized System (OECD-hazard).

**In vivo Activity**

**Table 10 Body Weight (gms)**

S. No.	Group	Body Weight (gms)						
		0 day	3 day	7 day	10 day	14 day	17 day	21 day
I	Normal	160.2±16.082	157±16.082	156±14.725	156.52±16.605	157±17.010	158.3±12.85	158.4±16.082
II	Inducer	232±38.742	233.33±37.112	225±42	230.66±41.525	218±47.791	227±45.508	237±47.031
II I	Standard	148.66±11.590	122.33±10.115	127.66±10.785	150.33±7.63	164.33±8.621	162.33±7.023	157±7
I V	Test Sample (nansponges gel containing isolated compound)	196±13	188.33±12.096	191.33±11.060	189.66±9.073	193.33±11.7	201.66±8.736	201.33±8.326

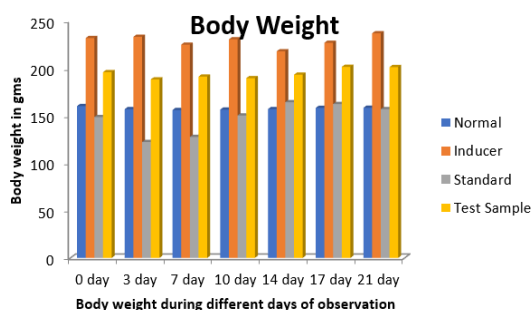


**Figure 11 Body Weight Assessment**

**Wound contraction studies**

Wound contraction is another parameter used to assess wound healing. Significant wound contraction was shown in Table 11.

**Table 11 Percentage wound closure in various treatment groups**

Sr. No	Formulation	Area of wound during different days of observation (%)					
		3 day	7 day	10 day	14 day	17 day	21 day
1	Normal	10.32±2.564	21.74±6.327	32.98±25.213	50.52±18.231	66.51±5.897	75.11±7.663
2	Inducer	19.77±18.146	36.33±26.974	64.88±12.056	86.566±5.975	93.51±0.436	96.39±3.11
3	Standard (Cipladine Gel)	23.98±14.461	31.49±14.085	72.00±3.275	91.14±7.663	96.51±1.697	98.88±1.928
4	Nanosponges Gel (Methyl ferulatenanosponges)	29.77±17.256	50.61±20.227	76.55±13.101	95.56±5.161	97.75±3.891	98.86±1.962

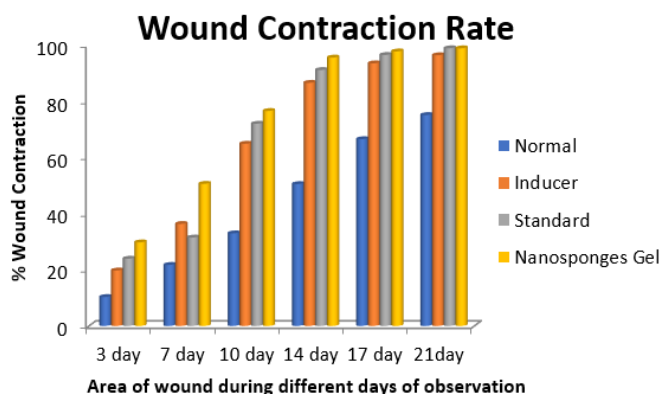


**Figure 12 Evaluation of wound healing activity**

## Images of wound closure

Table 12 Images of wound closure in various treatment groups

Group	0 Day	3 Day	7 Day	10 Day	14 Day	17 Day	21 Day
Normal							
Inducer							
Standard (1% w/w Cipladine Gel)							
Nanosponges gel (1% w/wMethylferulatenanosp onges)							

The discussion of the study's findings highlights notable observations regarding body weight fluctuations and wound contraction as indicators of health and wound healing efficacy. The body weight assessment results detailed in Table 10 reveal distinct trends among the groups. The normal group (Group I) exhibited consistent body weight stability, with minor variations across the 21-day period, suggesting typical physiological maintenance without significant external influences. In contrast, the inducer group (Group II) presented a higher baseline weight, with variations observed over time, potentially reflecting metabolic or stress-related changes induced by external factors. The standard treatment group (Group III) initially experienced a marked decline in body weight by day 3, likely due to initial treatment effects or physiological adaptation, by a gradual recovery, achieving close-to-normal weights by day 14. Similarly, the test sample group (Group IV) showed an initial weight decrease by day 3, followed by recovery and consistent weight maintenance, indicating tolerability and potential therapeutic efficacy of the test sample.

The wound contraction analysis, as illustrated in Table 11, further underscores the therapeutic characteristics of the tested formulations applied topically at a dose of (200mg/rat) once a day. The normal group did not show any significant wound

contraction, which was expected due to the lack of intervention. The inducer group displayed progressive wound closure, with significant contraction by day 14 ( $86.57\% \pm 5.975$ ) and nearly complete closure by day 21 ( $96.39\% \pm 3.11$ ). The standard group treated with Cipladine Gel achieved superior results, with 72% contraction by day 10 and near-complete healing ( $98.88\% \pm 1.928$ ) by day 21. Remarkably, the nanosponge gel formulation demonstrated the most effective wound contraction, achieving significant closure by day 10 ( $76.55\% \pm 13.101$ ) and matching the outcomes of the standard treatment by day 21 ( $98.86\% \pm 1.962$ ). These results underscore the enhanced wound healing efficacy of the nanosponge gel, likely attributable to its formulation, which promotes sustained release and targeted activity of isolated compound.

Graphical representations of body weight and wound healing trends further validate these findings, showcasing the differential effects of treatments. Overall, the study demonstrates that the nanosponge gel not only supports effective wound healing but also maintains body weight stability, highlighting its properties as a superior therapeutic formulation compared to standard treatments. Images of wound closure would have documented the visual progress of healing across the treatment groups over the observation period.

**CONCLUSION:**

The present investigation successfully formulated and evaluated nanosponges loaded with an isolated compound from *Launaea pinnatifida* for wound healing applications. The nanosponge-based gel exhibited excellent physicochemical properties, stability, safety, and significant wound healing efficacy *in vivo*, with results comparable to standard treatment. The enhanced performance can be attributed to the antioxidant, antimicrobial, and anti-inflammatory activities of the isolated compound, combined with the controlled-release potential of the nanosponge delivery system. Overall, this novel formulation provides strong evidence for the therapeutic potential of *Launaea pinnatifida* in wound management and highlights nanosponges as a promising drug delivery platform for plant-derived bioactives.

## REFERENCE

1. Ahmed MM, Fatima F, Anwer MK, Ibnouf EO, Kalam MA, Alshamsan A, Aldawsari MF, Alalawi A, Ansari MJ. Formulation and *in vitro* evaluation of topical nanosponge-based gel containing butenafine for the treatment of fungal skin infection. Saudi Pharm J. 2021 May;29(5):467-477. doi: 10.1016/j.jsps.2021.04.010. Epub 2021 Apr 27. PMID: 34135673; PMCID: PMC8180615.
2. Alashqar M, Goldstein N. Caffeine in the treatment of atopic dermatitis and psoriasis: a review. From Gene to Clinic International Congress, London: Psoriasis; 2017.
3. Aldawsari, M. F., Lau, V. W., Babu, R. J., Arnold, R. D., & Platt, S. R. (2018). Pharmacokinetic evaluation of novel midazolam gel formulations following buccal administration to healthy dogs. American Journal of Veterinary Research, 79(1), 73-82.
4. Anand, S., Pandey, P., Begum, M. Y., Chidambaram, K., Arya, D. K., Gupta, R. K., ...&Rajinikanth, P. S. (2022). Electrospun biomimetic multifunctional nanofibers loaded with methyl ferulatefor enhanced antimicrobial and wound-healing activities in STZ-Induced diabetic rats. Pharmaceuticals, 15(3), 302.
5. Anand, U., Tudu, C. K., Nandy, S., Sunita, K., Tripathi, V., Loake, G. J., ...&Proćków, J. (2022). Ethnodermatological use of medicinal plants in India: From ayurvedic formulations to clinical perspectives—A review. Journal of ethnopharmacology, 284, 114744.
6. Bhavana, P., Gottumukkala, S. N. V. S., Penmetsa, G. S., Ramesh, K. S. V., Kumar, P. M., &Meghana, M. (2023). Clinical evaluation of periosteal pedicle flap in the treatment of gingival recessions for esthetic root coverage: A randomized controlled clinical trial. Journal of Indian Society of Periodontology, 27(1), 76-81.
7. Bursal, E., & Köksal, E. (2011). Evaluation of reducing power and radical scavenging activities of water and ethanol extracts from sumac (*Rhus coriaria* L.). Food Research International, 44(7), 2217-2221.
8. Danaei M., Dehghankhold M., Ataei S., Hasanzadeh Davarani F., Javanmard R., Dokhani A., Khorasani S., Mozafari M.R. Impact of particle size and polydispersity index on the clinical applications of lipidic nanocarrier systems. Pharmaceuticals. 2018; 10:1–17. doi: 10.3390/pharmaceutics10020057.
9. Girigoswami, A., & Girigoswami, K. (2022). Versatile applications of nanosponges in biomedical field: a glimpse on SARS-CoV-2 management. BioNanoScience, 12(3), 1018-1031.
10. Gurtner, G. C., Werner, S., Barrandon, Y., & Longaker, M. T. (2008). Wound repair and regeneration. Nature, 453(7193), 314-321.
11. Habtemariam, A. B., & Kereta, A. K. (2020). Chromium (III) oxide nanostructures synthesized from Vernonia amygdalina leaves extract. Lett Appl NanoBioSci, 10, 1856-1861.
12. Jena, S., Ray, A., Banerjee, A., Sahoo, A., Nasim, N., Sahoo, S., ... & Nayak, S. (2017). Chemical composition and antioxidant activity of essential oil from leaves and rhizomes of Curcuma angustifolia Roxb. Natural Product Research, 31(18), 2188-2191.
13. Khan, M. A., Srivastava, V., Kabir, M., Samal, M., Insaf, A., Ibrahim, M., ... & Ahmad, S. (2021). Development of synergy-based combination for learning and memory using *in vitro*, *in vivo* and TLC-MS-bioautographic studies. Frontiers in Pharmacology, 12, 678611.
14. Khosravi-Darani, K., Gomes da Cruz, A., Shamloo, E., Abdimoghaddam, Z., & Mozafari, M. R. (2019). Green synthesis of metallic nanoparticles using algae and microalgae. Letters in applied nanoBioScience, 8(3), 666-670.
15. Kopel, J., McDonald, J., &Hamood, A. (2022). An assessment of the *in vitro* models and clinical trials related to the antimicrobial activities of phytochemicals. Antibiotics, 11(12), 1838.
16. Kumar, M., Patel, A. K., Shah, A. V., Raval, J., Rajpara, N., Joshi, M., & Joshi, C. G. (2020). First proof of the capability of wastewater surveillance for COVID-19 in India through detection of genetic material of SARS-CoV-2. Science of The Total Environment, 746, 141326.
17. Moin, Afrasim, NK FamnaRoohi, Syed Mohd Danish Rizvi, Syed Amir Ashraf, Arif Jamal Siddiqui, Mitesh Patel, S. M. Ahmed, D. V. Gowda, and Mohd Adnan. "Design and formulation of polymeric nanosponge tablets with enhanced solubility for combination therapy." RSC advances 10, no. 57 (2020): 34869-34884.
18. Osmani RAM, Bhosale RR, Hani U, Vaghela R, Kulkarni PK. Cyclodextrin based nanosponges: impending carters in drug delivery and nanotherapeutics. Curr Drug Ther. 2015;10(1):3–19
19. Patel, Diya, Panchal Diya, Patel Kunj, Prof. Dalwadi Mitali, Dr. Upadhyay Umesh , (2022), "A Review on UV Visible Spectroscopy", International Journal of Creative Research Thoughts (IJCRT), 2320-2882.
20. Patel, K., Robertson, E., Kwong, A. S., Griffith, G. J., Willan, K., Green, M. J., ... &Katikireddi, S. V. (2022). Psychological distress before and during the COVID-19 pandemic among adults in the United Kingdom based on coordinated analyses of 11 longitudinal studies. JAMA Network open, 5(4), e227629-e227629.
21. Rahamathulla, M., HV, G., Veerapu, G., Hani, U., Alhamhoom, Y., Alqahtani, A., &Moin, A. (2020). Characterization, optimization, *in vitro* and *in vivo* evaluation of simvastatin proliposomes, as a drug delivery. AAPS PharmSciTech, 21, 1-15.
22. Sahu, P. K., Ramiseti, N. R., Cecchi, T., Swain, S., Patro, C. S., & Panda, J. (2018). An overview of experimental designs in HPLC method development and validation. Journal of pharmaceutical and biomedical analysis, 147, 590-611.
23. Srivastava Nishi, Singh Arti, Kumari Puja, Jay Hind Nishad, Gautam Veer Singh, Yadav Monika, Bharti Rajnish, Kumar Dharmendra, Kharwar Ravindra N., (2021), "Advances in extraction technologies: isolation and purification of bioactive compounds from biological materials", Natural Bioactive Compounds: Technological Advancements, Elsevier Inc., 409-425.
24. Tiwari, K., & Bhattacharya, S. (2022). The ascension of nanosponges as adrug delivery carrier: preparation, characterization, and applications. Journal of Materials Science: Materials in Medicine, 33(3), 28.
25. Zia, F., Zia, K. M., Tabasum, S., Khosa, M. K., & Zuber, M. (2020). Preparation of hydroxyethyl cellulose/halloysite nanotubes graft polylactic acid-based polyurethane bionanocomposites. International journal of biological macromolecules, 153, 591-599.